Molecular Electronics

Synthesis of Diode Molecules and Their Sequential Assembly to Control Electron Transport**

*Ping Jiang, Gustavo M. Morales, Wei You, and Luping Yu**

Molecular electronics was envisioned to be the ultimate solution to the limit predicted by Moore's law for microelectronic chips. Since Aviram and Ratner proposed the original idea (the AR model) about molecular diodes,[1] many molecules that behave as wires,[2] diodes,[3] and switches[4] have been synthesized and characterized. Despite this progress, however, many challenges still remain to producing true molecular devices. For example, serious challenges exist for the assembly of these molecules into electric circuits, and reliable measurements on electron transport of single molecules in a true circuit configuration are still rare. Although the realization of single molecular electronics cannot be reached in one step, one of the most important steps towards real molecular devices is to control the functions of molecular components, such as rectification, in two-terminal molecules. A number of diode molecules developed by different research groups were based on the AR model and showed possible rectifying effects. However, these molecules could not be assembled into two-terminal circuits with a controlled direction of current flow. Herein, we report that the rectifying direction of diode molecules can be controlled in a two-terminal circuit configuration through a sequential assembly process. To the best of our knowledge, this is the first example in which the electron transport is controlled by the orientation of diode molecules between two electrodes.[5]

Recently, we reported that simple conjugated diblock co-oligomers exhibit pronounced rectification effects.[6] These p-n junction types of molecules incorporate an electron-rich dithiophene segment and an electron-deficient dithiazole segment. These molecular diodes contain only one thiol terminus, which limits their ability to be incorporated between two gold electrodes; it is necessary to equip this thiophene–thiazole diblock oligomer with two different terminal thiol groups that can be sequentially connected to gold electrodes, thereby enabling the molecular orientation between the two electrodes to predetermine the rectifying direction. We synthesized two thiophene–thiazole diblock oligomers with two different thiol-protected end groups. The orientation of the diblock structure between the gold electrodes was controlled through a sequential deprotection and immobilization procedure (deprotection a/self-assembly/deprotection b/adding Au nanoparticles). It was found from electron-transport studies that the rectifying effect of the resulting assembly was indeed controlled by the orientation of the molecules.

The synthetic procedure for the thiophene–thiazole diblock molecule was reported previously.[6] Introducing another thiol group into the compound proved to be not feasible because of tautomerism between the thiol and thione forms. However, we found that thiolation at the 5-position in the thiazole molecule could be achieved. Thus, compounds **6** and **13** were designed and synthesized (Scheme 1). The two thiol-protection groups used are cyanoethyl ($-SCH_2CH_2CN$, CNE) and trimethylsilylethyl ($-SCH_2CH_2SiMe_3$, TMSE). The former can be readily cleaved to the free thiol under basic conditions while the latter is stable even under very basic conditions, such as butyllithium, but labile to fluoride-mediated cleavage.[7] Our synthetic strategy was to take advantage of the inertness of the TMSE protecting group to basic conditions and incorporate it at the beginning, and then add the CNE protection group later in the synthesis. The TMSE-protected thio group was first attached to the dithiophene unit through the dithiophene iodide **1** by using a general method for formation of an aryl–sulfur bond in which a copper(I) salt is used as a catalyst.[8] The diblock molecule **5** with a TMSE protecting group was prepared by Stille coupling of **3** with the dithiazole block **4**. The last step was to introduce the CNE protecting group at the other end to form **6** by using a previously used procedure.[6b]

Originally we planned to deprotect the thio groups in compound **6** by two different sequences so that the diode molecule could be immobilized onto electrodes with different orientations. Experiments showed that initial cleavage of the TMSE group would also simultaneously eliminate the CNE group. However, cleavage of the CNE group first, worked well with the TMSE group remaining intact. Thus, the sequential deprotection procedure (cleavage of the CNE group first and then the TMSE group) was applied. Compound **13** was then synthesized to enable the reverse molecular orientation to be realized between the electrodes. Compound **13** has a similar diblock structure to compound **6**, but with the two different thio-protection groups switched in positions (Scheme 1). Since it is difficult to functionalize the 2-position of the dithiazole unit after protecting the thio group at the 5′-position with TMSE, we chose first to couple dithiazole **4** with one thiophene unit protected at its 2-position to form compound **8**, then attach the TMSE protecting group by using the same coupling reaction described above. Finally another thiophene unit with a built-in CNE-protected thio group was connected through a Stille coupling reaction to make compound **13**. The ^1H and ^{13}C spectra of the compounds are consistent with the expected structures, and the mass spectra show a signal for M^+ at about m/z 604.9 for both **6** and **13**.

The orientation of the diblock structure between gold electrodes was controlled through a sequential deprotection

[*] P. Jiang, G. M. Morales, W. You, Prof. L. Yu
Department of Chemistry and James Franck Institute
The University of Chicago
5735 South Ellis Avenue, Chicago, Illinois, 60637 (USA)
Fax: (+1) 773-702-0805
E-mail: lupingyu@midway.uchicago.edu

[**] We thank the financial support from the National Science Foundation, the NSF MRSEC program at The University of Chicago, and AFOSR. Partial support for this research was provided by the UC-Argonne Nanoscience Consortium.

Supporting information for this article is available on the WWW under http://www.angewandte.org or from the author.

 DOI: 10.1002/ange.200460110

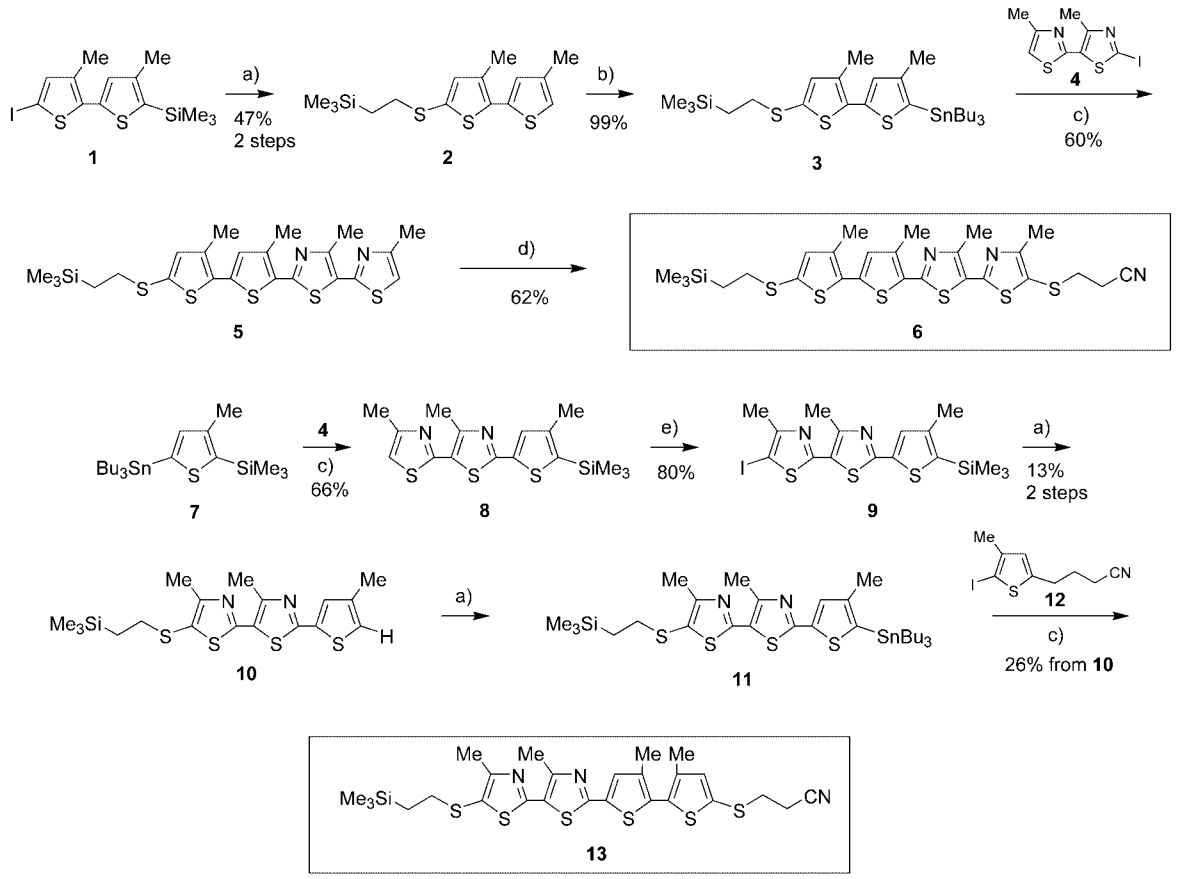

Scheme 1. Syntheses of compound **6** and **13**. a) 1. $Me_3SiCH_2CH_2SH$, CuI, NaO*t*Bu, neocuproine, toluene, 110 °C; 2. TFA; b) 1. *n*BuLi, −78 °C; 2. Bu_3SnCl; c) $[Pd_2(dba)_3]$, PPh_3, Cu_2O, DMF, 130–135 °C; d) 1. *n*BuLi, −78 °C; 2. S_8; 3. $BrCH_2CH_2CN$; e) 1. *n*BuLi, THF, −78 °C; 2. I_2. TFA = trifluoroacetic acid, dba = *trans*,*trans*-dibenzylideneacetone.

and immobilization procedure (deprotection a/self-assembly/deprotection b/add Au nanoparticles) as described in Scheme 2. First, the CNE protecting group was cleaved in situ with sodium ethoxide/ethanol to form a free thiol, and the target molecules were then self-assembled onto the gold substrate. Then the TMSE-protecting group was cleaved with a solution of TBAF in THF and treated with freshly made gold nanoparticles (NP). Thus the diode molecules were connected at both ends to gold electrodes and ready for the electron-transport study. The assemblies **A1** and **A2**, prepared from molecule **6** and **13**, respectively, are shown in Scheme 2.

An investigation of the charge-transport properties of single molecules necessitates monolayers with isolated diode molecules. We utilized a dodecanethiol self-assembled monolayer (DDT SAM) on an Au(111) substrate into which the molecules **6** and **13**, were inserted. Figure 1a shows the STM image of the highly ordered structure of a DDT SAM on an Au(111) surface. High-resolution images (inset in Figure 1a) reveal a hexagonal packing, with an average distance between the nearest and next-nearest-neighbor spacing (represented by *a* and *b*, respectively) of approximately 0.5 and 0.9 nm, which correspond to a characteristic $(\sqrt{3}\times\sqrt{3})$ R30° absorbate overlayer on Au(111).[9] Figure 1b shows an STM image taken on the DDT SAM after insertion of **6**. The bright spot (indicated by a circle) is the constant-current STM image of **6** with the TMSE-protected thio group on the top. The images are reproducible over many scans. The intensity of the bright spots changes sporadically in agreement with the stochastic behavior reported for single molecules inserted in an alkanethiol SAM.[10] The shape and size of the spots are constant and have an average size of about 1.8 nm, which is similar to other single molecules inserted in an alkyl thiol matrix.[11] The bright spots are probably single molecules, but we cannot rule out the possibility of the formation of aggregates. According to literature data the orientation of DDT is defined by a tilt angle of 30°.[9] After removal of the TMSE protecting groups, Au NPs were attached to the exposed terminal thiol groups. Figure 1c shows the STM image of the resulting Au assembly **A1**. The apparent diameter of the Au NP is in the range 9–11 nm. A separate TEM micrograph of the NP showed an average diameter of 8 nm.[12] The enlargement in the size of the single molecules and NPs can be attributed to the combination of electronics factors and tip-convolution effects. Control experiments showed that the nanoparticles were indeed attached to the molecules after cleavage of the TMSE group. First, there were no nanoparticles observed on the STM images of samples prepared under the same conditions without cleavage of the TMSE group or in the absence of inserted target molecules.

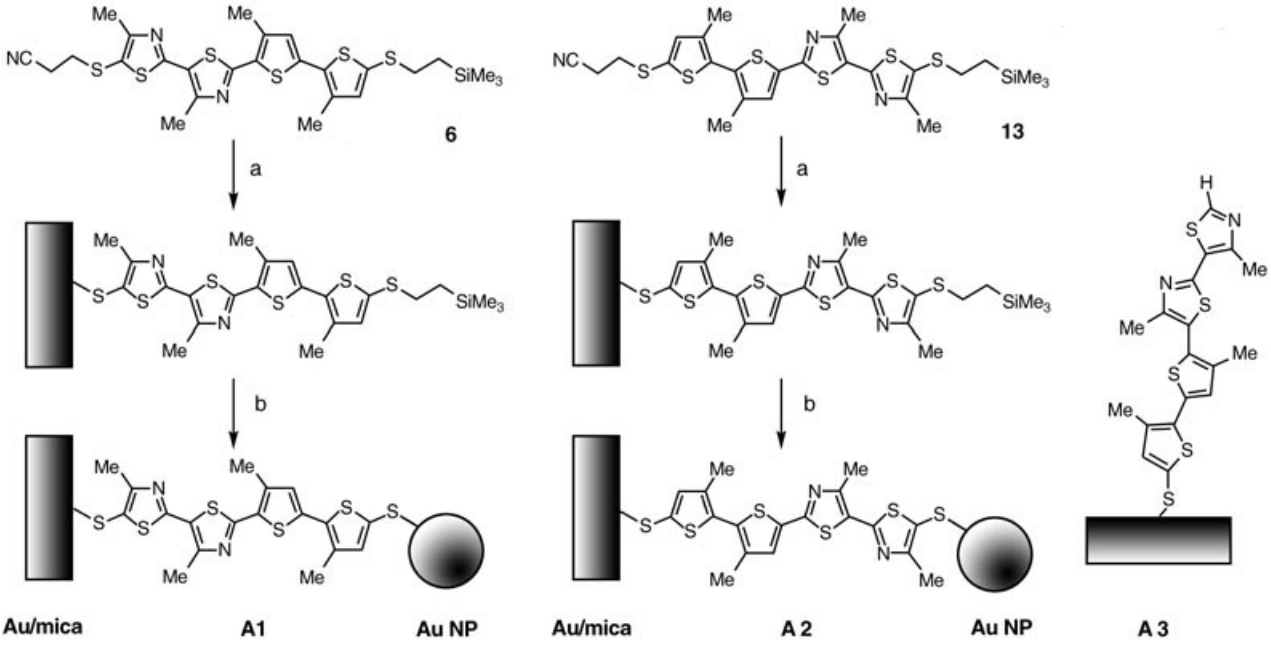

Scheme 2. Preparation of assemblies **A1** and **A2**. a) NaOEt, THF, gold substrate; b) TBAF, THF, Au nanoparticles. For assembly **A3** see ref [5b]. TBAF = tetrabutylammonium fluoride.

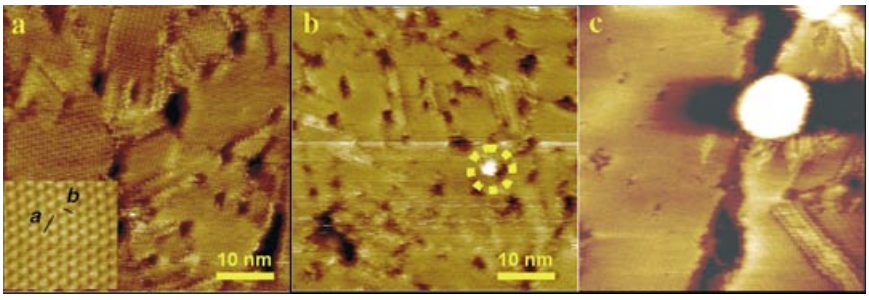

Figure 1. Constant-current STM topography of a dodecanethiol SAM on Au(111)/mica, before (a) and after (b) the insertion of **6**; the molecule is shown as a bright spot and indicated by a circle. c) The image of the surface after attachment of Au nanoparticle to the top termini of **6**. The area shown is 50×50 nm^2, STM imaging conditions: $V_{bias} = +1.0$ V, $I_t = 1$ pA.

Secondly, the density of the nanoparticles observed after step b in Scheme 2 was comparable to that of the bright spots from the molecules with the TMSE-protected thio group after step a in Scheme 2.

Further evidence for the sequential deprotection process was obtained from grazing incidence FTIR. Figure 2 shows the IR spectra in the CH stretching region for a monolayer of **6** following the sequential deprotection. The transmission spectrum of **6** on a KBr plate is shown for comparison (trace a). The inset spectra show the CN stretching region, where disappearance of the CN absorption was clearly observed after the first deprotection step, namely cleavage of the CNE group. The absorption from the CH_2 unit (νCH_2^s symmetric stretching vibration) of the TMSE group remains (indicated by an arrow in trace b),[13] thus indicating the TMSE group was intact. After the second deprotection step (cleavage of the TMSE group), this absorption from the TMSE group disappeared accordingly (trace c).

The electron-transport properties of assemblies **A1** and **A2** were investigated by scanning tunneling spectroscopy (STS). It has been demonstrated that gold NPs can be immobilized on the surface thiol groups in symmetrical alkyl dithiol monolayers assembled on a Au substrate and *I*/*V* properties of the assembly can be readily measured by scanning probe microscopy.[14] Figure 3 summarizes the averaged *I*/V data for assemblies **A1** and **A2** (Scheme 2). The gap conditions used to define the tip–sample separation are −0.5 and −0.1 nA at −1.5 V, respectively. The STS spectra for **A1** clearly showed asymmetric *I*/V behavior, with higher current at a negative bias potential than at a positive one. The average rectification ratio (RR) is 0.19:1 (for easy comparison, 1/RR was used in Figure 3a), where RR is defined as $RR = I(+1.5\text{ V})/I(-1.5\text{ V})$.[15] Opposite rectifying behaviors were found for assembly **A2**, with an average RR value of 4.8:1. The inset histograms show the statistical distribution of 1/RR for **A1** and RR for **A2** for the different NPs measured, thus demonstrating the reproducibility of the *I*/V curves for different NPs on the SAM monolayer. The RR range is 2:1–7:1 for **A1** while the 1/RR range for **A2** is 3:1–7:1. The ranges in both cases can be attributed to different orientations and conformations of the molecules in the SAM defects.[10a,16] The statistical histogram analyses were based on measurements taken on about 50 different immobilized single Au NPs for each assembly. The *I*/*V* data for each NP is the average of about 100 individual *I*/*V* curves, each of which is composed of 256 points, while each point has been averaged 3–5 times by the software.

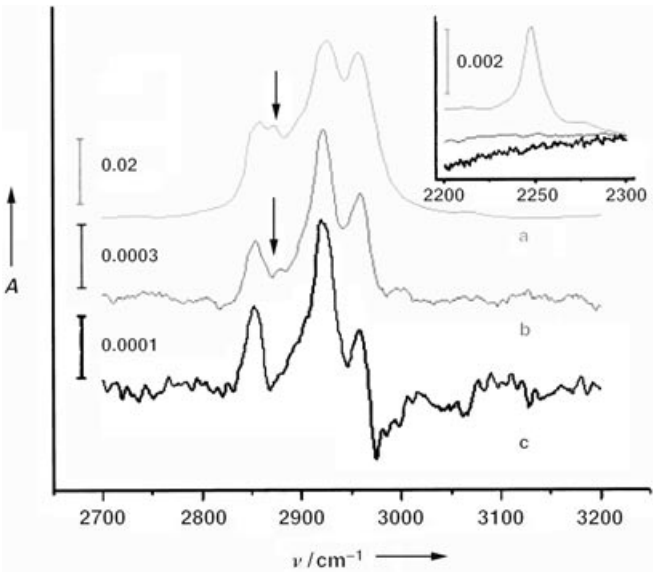

Figure 2. Grazing incidence FTIR spectra in the CH stretching region of a) pure compound **6** in KBr, b) a monolayer of compound **6** on Au after deprotection of the CNE group, and c) after cleavage of the TMSE group. The inset spectra shows the CN stretching region.

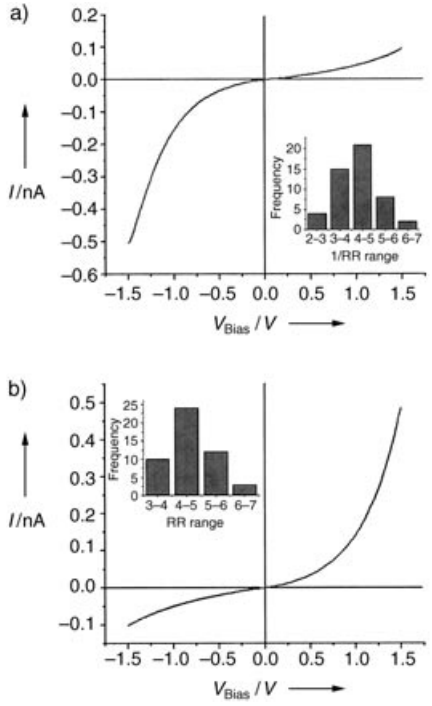

Figure 3. Averaged *I*/*V* curves measured over approximately 50 different gold nanoparticles at $V_{bias} = -1.5$ V for a) **A1** ($I_t = -0.5$ nA) and b) **A2** ($I_t = -0.1$ nA).

We also changed the current set points (distance between the STM tip and the Au NP) to investigate the behavior of the junction under different gap conditions. Figure 4 shows the *I*/*V* curves obtained at different current set points for **A1** and **A2**. The opposite asymmetric *I*/*V* behaviors for **A1** and **A2** were observed consistently with various current set points. Although the interplay of two junctions together with the

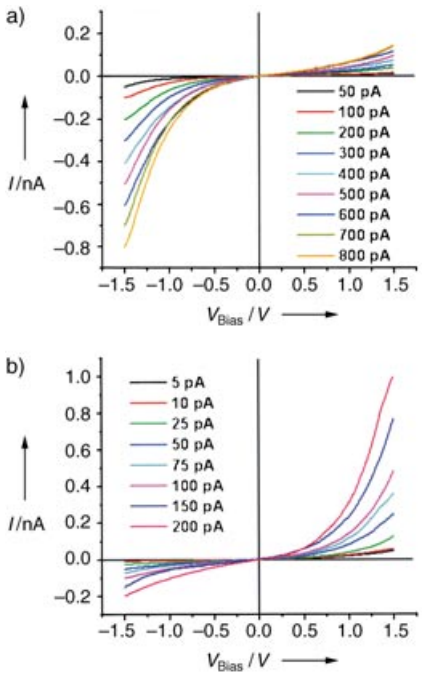

Figure 4. *I*/*V* data taken at different current set points for a V_{bias} of −1.5 V for: a) **A1** and b) **A2**.

charging of the NP can change the symmetry of the *I*/*V* curve,[17] the contribution should be always in the same direction. In our case the opposite asymmetry between **A1** and **A2** ruled out any significant contribution from such an effect.

Since the opposite rectifying behavior for **A1** and **A2** also rules out any contribution in the asymmetry originating from the measurement setup, the rectifying effect observed should be an intrinsic property of the molecules. Although the position of one methyl group on one thiophene ring was different in compounds **6** and **13**, which may affect the twist angle of the conjugation and thus electron delocalization, we believe that the determining factor is the dipole orientation of the thiophene–thiazole diblock rather than the slight difference in the position of the methyl group. The results are consistent with our previous results obtained from **A3** (Scheme 2). Assembly **A3** has the same dipole orientation as **A2**. Preliminary calculations at the HF/G-31G level showed that the component along the molecule axis is 1.68 and 1.54 D for molecules **6** and **13**, respectively.

In summary, we have synthesized new diode molecules with two different terminal thiol groups that are protected differenlt. Sequential deprotection of these groups enables us to assemble the diode molecules with controlled orientations between two gold electrodes. By manipulating the orientations of the diode molecules between electrodes we were able to control the rectification directions. Reproducible results from STS studies clearly support the concept of using diblock conjugated oligomers with opposite electronic demands for a rectifying effect. The results also indicate that the dipole moments may play an important role in determining the rectifying direction and ratio.

Experimental Section

5: *n*BuLi (1.2 mL, 1.6 M in hexanes) was added dropwise to a solution of **2** (489 mg, 1.5 mmol) in dry THF (15 mL) cooled at −78 °C. The resulting solution was allowed to warm to room temperature over 30 minutes, recooled to −78 °C, and quenched with tributyltin chloride (814 mg, 2.5 mmol). The mixture was stirred at room temperature for 4 h, poured into aqueous sodium carbonate solution, and extracted with diethyl ether. The combined organic extracts were washed with brine, dried (Na_2SO_4), and the solvent was removed in vacuo. The crude organostannane intermediate **3** was obtained in almost quantitatively yield (monitored by ^{1}H NMR spectroscopy). This crude product of **3** and compound **4** (483 mg, 1.5 mmol) were dissolved in anhydrous DMF (20 mL) and a mixture of $[Pd_2(dba)_3]$ (30 mg, 0.03 mmol), PPh_3 (60 mg, 0.23 mmol), and Cu_2O (65 mg, 0.45 mmol) were added in one portion. The resulting mixture was heated at 130–135 °C for 12 h, and then was cooled to room temperature. The DMF was then removed under high vacuum, $CHCl_3$ was added to the residue, and the resulting mixture was filtered through a pad of silica gel. The crude product was purified by column chromatography (silica gel, hexane/ethyl acetate, 10:1, v/v) to afford **5** (468 mg, 60 %) as a pink solid. ^{1}H NMR (500 MHz, $CDCl_3$): $\delta = 0.01$ (s, 9H, $SiMe_3$), 0.94 (t, $J = 8.5$ Hz, 2H, CH_2), 2.37 (s, 3H, Me), 2.47 (s, 3H, Me), 2.49 (s, 3H, Me), 2.68 (s, 3H, Me), 2.88 (t, $J = 8.5$ Hz, 2H, CH_2), 6.82 (s, 1H, Ar-H), 6.88 (s, 1H, Ar-H), 6.91 ppm (s, 1H, Ar-H); ^{13}C NMR (125 MHz, $CDCl_3$): $\delta = -1.8$, 15.8, 16.5, 17.0, 17.5, 17.6, 34.8, 113.5, 126.7, 128.4, 129.4, 131.5, 132.2, 133.9, 135.0, 136.8, 138.0, 150.7, 153.2, 158.1, 158.9 ppm.

6: *n*BuLi (0.4 mL, 1.6 M in hexanes) was added dropwise to a solution of compound **5** (260 mg, 0.5 mmol) in dry THF (10 mL) cooled at −78 °C. The resulting solution was allowed to warm to room temperature for 20 min, recooled to −78 °C, and quenched with sulfur powder (22.4 mg, 0.7 mmol). The mixture was warmed to 0 °C for 20 min, then recooled to −78 °C, and treated with a solution of 3-bromopropionitrile (113 mg, 0.84 mmol) in THF (2 mL). The mixture was stirred at room temperature overnight, poured into water, and extracted with diethyl ether. The combined organic extracts were washed with brine, dried (Na_2SO_4), and the solvent was removed in vacuo. The crude product was purified on silica gel (hexane/ethyl acetate, 4:1, v/v) to afford **6** (202 mg, 62 %). ^{1}H NMR (500 MHz, $CDCl_3$): $\delta = 0.02$ (s, 9H, $SiMe_3$), 0.97 (t, $J = 8.5$ Hz, 2H, CH_2), 2.41 (s, 3H, Me), 2.54 (s, 3H, Me), 2.56 (s, 3H, Me), 2.66 (t, $J = 7.0$ Hz, 2H, CH_2), 2.71 (s, 3H, Me), 2.91 (t, $J = 8.5$ Hz, 2H, CH_2), 3.02 (t, $J = 7.0$ Hz, 2H, CH_2), 6.87 (s, 1H, Ar-H), 6.97 ppm (s, 1H, Ar-H); ^{13}C NMR (125 MHz, $CDCl_3$): $\delta = -1.8$, 15.5, 15.9, 16.5, 17.4, 17.7, 18.0, 33.3, 34.7, 117.5, 119.9, 126.4, 129.3, 130.8, 133.1, 134.1, 135.2, 136.6, 137.7, 138.5, 151.9, 159.0, 159.6, 160.4 ppm; $\lambda_{max} = 421$ nm; MS (CI): calcd mass for $C_{26}H_{31}N_3S_6Si$: m/z 605.06; found: m/z 605.8 $[M+1]^+$.

Further experimental details for the synthesis of all other compounds, assembly preparation, STM, STS, and FTIR measurements can be found in the Supporting Information.

Received: March 24, 2004 [Z460110]

Keywords: electron transport · molecular electronics · monolayers · self-assembly

[1] A. Aviram, M. Ratner, *Chem. Phys. Lett.* **1974**, *29*, 277–283.
[2] J.-P. Launay, *Chem. Soc. Rev.* **2001**, *30*, 386–397.
[3] R. M. Metzger, *Chem. Rev.* **2003**, *103*, 3803–3834.
[4] *Molecular Switches* (Ed.: B. L. Feringa), Weinheim, Chichester, Wiley-VCH, **2001**.
[5] During the preparation of this manuscript, the use of two different protection groups to orientate the molecules on gold wires was reported: S. K. Pollack, J. Naciri, J. Mastrangelo, C. H. Patterson, J. Torres, M. Moore, R. Shashidhar, J. G. Kushmerick, *Langmuir* **2004**, *20*, 1838–1842.
[6] a) M.-K. Ng, L. Yu, *Angew. Chem.* **2002**, *114*, 4750–3753; *Angew. Chem. Int. Ed.* **2002**, *41*, 3598–3601; b) M.-K. Ng, D.-C. Lee, L. Yu, *J. Am. Chem. Soc.* **2002**, *124*, 11862–11863.
[7] M. B. Anderson, M. G. Ranasinghe, J. T. Palmer, P. L. Fuchs, *J. Org. Chem.* **1988**, *53*, 3127–3129.
[8] C. G. Bates, R. K. Gujadhur, D. Venkataraman, *Org. Lett.* **2002**, *4*, 2803–2806.
[9] a) C. A. Widring, C. A. Alves, M. D. Porter, *J. Am. Chem. Soc.* **1991**, *113*, 2805–2810; b) C. A. Alves, E. L. Smith, M. D. Porter, *J. Am. Chem. Soc.* **1992**, *114*, 1222–1227.
[10] a) Z. J. Donhauser, B. A. Mantooth, K. F. Kelly, L. A. Bumm, J. D. Monnell, J. J. Stapleton, D. W. Price, Jr., A. M. Rawlett, D. L. Allara, J. M. Tour, P. S. Weiss, *Science* **2001**, *292*, 2303–2307; b) G. K. Ramachandran, T. J. Hopson, A. M. Rawlett, L. A. Nagahara, A. Primak, S. M. Lindsay, *Science* **2003**, *300*, 1413–1416; c) R. A. Wassel, R. R. Fuierer, N. Kim, C. B. Gorman, *Nano Lett.* **2003**, *3*, 1617–1620.
[11] P. S. Weiss, L. A. Bumm, T. D. Dunbar, T. P. Burgin, J. M. Tour, D. L. Allara, *Ann. N. Y. Acad. Sci.* **1998**, *852*, 145–168.
[12] D. I. Gittins, F. Caruso, *Angew. Chem.* **2001**, *113*, 3089–3092; *Angew. Chem. Int. Ed.* **2001**, *40*, 3001–3004.
[13] The assignment of this absorption band was made by a comparitive study of the IR spectra of different model compounds; for details see the Supporting Information.
[14] a) M. Dorogi, J. Gomez, R. Osifchin, R. P. Andres, R. Reifenberger, *Phys. Rev. B* **1995**, *52*, 9071–9077; b) D. I. Gittins, D. Bethell, D. J. Schiffrin, R. J. Nichols, *Nature* **2000**, *408*, 67–69; c) X. D. Cui, A. Primax, X. Zarate, J. Tomfohr, O. F. Sankey, A. L. Moore, T. A. Moore, D. Gust, G. Harris, S. M. Lindsay, *Science* **2001**, *294*, 571–574.
[15] R. M. Metzger, T. Xu, I. R. Peterson, *J. Phys. Chem. B* **2001**, *105*, 7280–7290.
[16] a) M. T. Cygan, T. D. Dunbar, J. J. Arnold, L. A. Bumm, N. F. Shedlock, T. P. Burgin, L. Jones II, D. L. Allara, J. M. Tour, P. S. Weiss, *J. Am. Chem. Soc.* **1998**, *120*, 2721–2732; b) S. Yasuda, T. Nakamura, M. Matsumoto, H. Shigekawa, *J. Am. Chem. Soc.* **2003**, *125*, 16430–16433; c) L. Patrone, S. Palacin, J. P. Bourgoin, J. Lagoute, T. Zambelli, S. Gauthier, *Chem. Phys.* **2002**, *281*, 325–332.
[17] A. E. Hanna, M. Tinkhan, *Phys. Rev. B* **1991**, *44*, 5919–5922.

